coatings

MDPI

Article

Preparation Process Optimization for Melamine Resin-Covered Pomelo Peel Flavonoid Antibacterial Microcapsules and Their Effect on Waterborne Paint Film Performance

Tingting Ding [1,2] and Xiaoxing Yan [1,2,*]

[1] Co-Innovation Center of Efficient Processing and Utilization of Forest Resources, Nanjing Forestry University, Nanjing 210037, China; dingtingting@njfu.edu.cn
[2] College of Furnishings and Industrial Design, Nanjing Forestry University, Nanjing 210037, China
* Correspondence: yanxiaoxing@njfu.edu.cn

Abstract: Pomelo peel is a natural substance with antibacterial properties. Its extraction process is simple, and the raw materials are abundant. Microcapsules were prepared using melamine resin as the wall material and pomelo peel flavonoids as the core material. The optimization of microcapsule preparation was explored by orthogonal and single-factor experiments. The findings indicated that the optimum process for the preparation of microencapsulation was a 0.12:1 mass ratio of core to wall material, 60 °C microencapsulation reaction temperature, 800 rpm microencapsulation reaction stirring speed, and 2% emulsifier concentration. On this basis, the microcapsules were applied to waterborne coatings at different levels, 0%, 3.0%, 6.0%, 9.0%, 12.0%, and 15.0%, respectively, to prepare paint films, and the properties of the paint films were tested and explored. The test showed that the microcapsules added to the waterborne paint film exhibited antibacterial activity while retaining good optical and mechanical properties. In comparison with *Escherichia coli*, the microcapsules had a greater antibacterial rate against *Staphylococcus aureus*. When the content of microcapsules was 6.0%, the general performance of the waterborne paint film was optimal. The antibacterial rate of the paint film against *Staphylococcus aureus* and *Escherichia coli* was 40.5% and 50.5%, respectively. The color difference was 3.28. The paint film had a certain elasticity area, the elongation at break was 10.8%, and the roughness was 1.75 μm. We successfully prepared microcapsules capable of improving the antibacterial performance of waterborne paint film, which expands the application field of waterborne coatings and provides a certain reference value for the antibacterial research of waterborne coatings.

Keywords: microcapsule; pomelo peel flavonoids; antibacterial properties; paint film

Citation: Ding, T.; Yan, X. Preparation Process Optimization for Melamine Resin-Covered Pomelo Peel Flavonoid Antibacterial Microcapsules and Their Effect on Waterborne Paint Film Performance. *Coatings* **2024**, *14*, 654. https://doi.org/10.3390/coatings14060654

Academic Editor: Maria Jose Fabra

Received: 21 March 2024
Revised: 6 May 2024
Accepted: 18 May 2024
Published: 21 May 2024

1. Introduction

In contemporary society, people's living conditions are constantly improving. People attach importance to the living environment, and the demand for a healthy life is becoming stronger and stronger. Microbial pollution produced in daily life has an impact on people's health [1–6]. Paint film is applied to the surfaces of household products that people directly have contact with in their daily lives. The paint film of household surfaces is an important carrier for the spread of bacteria, so improving the antibacterial characteristics of paint films is an effective means of blocking the indirect spread of bacteria. A waterborne coating is a new type of environmentally friendly coating using water as a solvent, reducing the use of organic solvents and lowering pollution. However, waterborne coatings also have problems, such as a lack of hardness and a singular function. Currently, research on the enhancement of waterborne coatings' antibacterial properties is relatively scarce, warranting further exploration [7–10]. The antibacterial function of coatings can significantly decrease the bacteria hosted on furniture, so that people's living space can be further optimized, and has

practical application value [11–14]. This demands a more in-depth study of the antibacterial function of coatings.

Microencapsulation is a preparation technique, in which a core material is covered within a wall material, that can be applied to the preparation of antibacterial agents [15–19]. Substances with antibacterial properties can be wrapped as a core material in this way, thereby stabilizing the core material and achieving a long-lasting antibacterial effect [20–25]. Preparing antibacterial agents into microcapsules and adding them to coatings can optimize the performance of the antibacterial agents and enhance the antibacterial function of the coatings, thus making it practical to optimize antibacterial preparation and enhance the function within the coatings. Melamine resin is a common microcapsule wall material with a simple manufacturing process and relatively low cost [26–30]. It has obvious advantages in the preparation of microcapsules. Melamine resin shows good film-forming performance, has stable chemical properties, and can be kept in a stable state in many cases, effectively protecting internal substances from external environment interference and controlling release ability, so as to realize the slow, sustained release of internal substances [31–34]. Tao et al. demonstrated the utility of melamine resin microcapsules for waterborne coatings by using melamine resin as a wall material [35].

Grapefruit peel is rich in resources. As a natural antibacterial agent, grapefruit peel extract has obvious antibacterial properties, and the extraction process is simple. The antibacterial mechanism is mainly related to active components such as flavonoids and volatile oil [36–39]. Flavonoids are a class of yellow pigments with the flavonoid 2-phenylchromenone as the parent nucleus. The flavonoid structure is shown in Figure 1, which includes the isomers of flavonoids and their hydrogenation and reduction products, i.e., a series of compounds with C6-C3-C6 as the basic carbon framework. Flavonoids are widely distributed in plants, and most of them combine with sugar to form glycosides in the form of sugar ligands. Pomelo peel contains mainly 5,7,4,-trihydroxyflavonoids and naringenin at the 7-position carbon [40–43]. These components have broad-spectrum antibacterial effects, which can effectively inhibit the growth of various bacteria and fungi, and have broad application prospects. Aichayawanich et al. used four organic solvents, namely, ethanol, dichloromethane, hexane, and ethyl acetate, to derive a crude grapefruit peel extract and proved that it could be used to inhibit *Staphylococcus aureus* [44]. Thavanapong et al. obtained grapefruit peel oil extracted by cold pressing, vacuum steam distillation, and supercritical carbon dioxide extraction, and used it to prove that grapefruit oil and grapefruit extract have quite good antibacterial activity against *Staphylococcus aureus* [45].

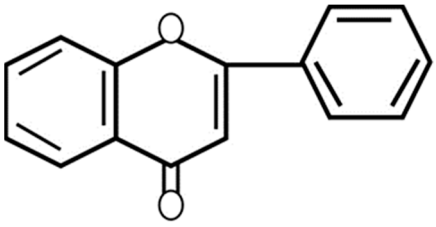

Figure 1. Flavonoid structure diagram.

Escherichia coli and *Staphylococcus aureus* are common bacteria. Therefore, this experiment was chosen to study the antibacterial properties of microcapsules against these two bacteria in waterborne paint films and to analyze the influence of various microcapsule contents on the comprehensive optical and mechanical characteristics of waterborne paint films. The antibacterial microcapsules were made from pomelo peel flavonoids covered with melamine resin. The coverage rate, yield, and morphology of the microcapsules were assessed and characterized by orthogonal and single-factor tests to determine the optimum technological parameters for microcapsule preparation. Waterborne paint film was prepared by adding microcapsules with different contents into waterborne topcoat, and the effects of different addition amounts on the macro- and micromorphology and properties

of the paint film were analyzed. The purpose is to ensure that the waterborne paint film has good optical and mechanical properties while enhancing its antibacterial properties.

2. Materials and Methods

2.1. Experimental Materials

Table 1 shows the experimental materials. The waterborne coatings used were waterborne acrylic varnishes from Jiangsu Himonia Technology Co., Ltd., Zhenjiang, China. Waterborne paint films were prepared using silicone molds of 50 mm × 50 mm × 10 mm. The materials required in the test also included polyethylene film measuring 40 mm × 40 mm × 0.08 mm and petri dishes with a diameter of 90 mm. The second-generation standard strains of *Escherichia coli* and *Staphylococcus aureus* were ATCC25922 and ACTT6538, which were obtained from the Beijing Biological Preservation Centre, Beijing, China. The pomelo peel used in this experiment was Guangxi Shatian Pomelo obtained from Beihai, China.

Table 1. Table of materials required for the experiment.

Material	Molecular Formula	M_W (g/mol)	CAS No.	Concentration (%)
Melamine	CH_4N_2O	60.06	57-13-6	99.0
Formaldehyde solution	-	-	-	37.0
Triethanolamine	$C_6H_{15}NO_3$	149.19	102-71-6	99.9
Citric acid monohydrate	$C_6H_{10}O_8$	210.14	5949-29-1	99.9
Sodium dodecyl benzene sulfonate	$C_{18}H_{29}NaO_3S$	348.48	25155-30-0	99.9
Anhydrous ethanol	C_2H_6O	46.07	64-17-5	99.9

2.2. Preparation of Microcapsules

In this study, the optimum preparation technique for manufacturing melamine resin microcapsules was investigated by setting up a four-factor, three-level orthogonal test, as shown in Table 2. Orthogonal tests were designed with four important influencing factors—namely, the mass ratio of core to wall materials, reaction temperature, stirring speed during the reaction, and emulsifier concentration during the emulsification process—and microcapsule samples were prepared and obtained with different parameters, as shown in Table 3. The yield, coverage, and morphological results of the obtained microencapsulated samples were comparatively analyzed to determine the optimal level of each factor in the microcapsule preparation process and the primary and subsidiary relationships of the influencing factors. The maximum influencing factors of microcapsule preparation were investigated, and a single-factor test was designed on the basis of the orthogonal test to further optimize the microcapsule preparation parameters and obtain the best preparation process for melamine resin-covered pomelo peel flavonoid antibacterial microcapsules. The experimental dosage of microcapsule preparation is shown in Table 4.

Table 2. Program design for orthogonal tests.

Level	Factor A $m_{(core\ material)}$: $m_{(wall\ material)}$	Factor B Temperature (°C)	Factor C Stirring Speed (rpm)	Factor D Emulsifier Concentration (%)
1	0.08:1	50	600	1
2	0.10:1	60	800	2
3	0.12:1	70	1000	3

Table 3. Specific parameters of the orthogonal test.

Sample	$m_{(core\ material)}$: $m_{(wall\ material)}$	Temperature (°C)	Stirring Speed (rpm)	Emulsifier Concentration (%)
1	0.08:1	50	600	1
2	0.08:1	60	800	2
3	0.08:1	70	1000	3
4	0.10:1	50	800	3
5	0.10:1	60	1000	1
6	0.10:1	70	600	2
7	0.12:1	50	1000	2
8	0.12:1	60	600	3
9	0.12:1	70	800	1

Table 4. Detailed dosage of materials.

Test Type	Sample	Melamine (g)	Formaldehyde Solution (g)	Wall Material (g)	Core Material (g)	Ethanol (mL)	Emulsifier (g)	Deionized Water (g)
Orthogonal test	1	10.00	19.30	17.13	1.37	12.33	2.74	271.26
	2	10.00	19.30	17.13	1.37	12.33	5.48	268.52
	3	10.00	19.30	17.13	1.37	12.33	8.22	265.78
	4	10.00	19.30	17.13	1.71	15.39	10.26	331.74
	5	10.00	19.30	17.13	1.71	15.39	3.42	320.58
	6	10.00	19.30	17.13	1.71	15.39	6.84	335.16
	7	10.00	19.30	17.13	2.06	18.54	8.24	403.76
	8	10.00	19.30	17.13	2.06	18.54	12.36	399.64
	9	10.00	19.30	17.13	2.06	18.54	4.12	407.88
Single-factor test	10	10.00	19.30	17.13	2.06	18.54	8.24	403.76
	11	10.00	19.30	17.13	2.06	18.54	8.24	403.76
	12	10.00	19.30	17.13	2.06	18.54	8.24	403.76
	13	10.00	19.30	17.13	2.06	18.54	8.24	403.76
	14	10.00	19.30	17.13	2.06	18.54	8.24	403.76

(1) Melamine resin wall material preparation: According to Table 4, a certain mass of 37% formaldehyde solution and a certain mass of melamine were mixed homogeneously according to a molar ratio of 3:1 and then added into deionized water. The pH value of the solution was adjusted to about 8 with triethanolamine. A magnetic stirrer was added and placed in an 80 °C thermostatic water bath, and the reaction was carried out at 800 rpm for 40 min. The reaction was continuously stirred to obtain the melamine resin wall prepolymer, which was cooled to room temperature and set aside.

(2) Pomelo peel flavonoid core emulsion preparation: Fresh pomelo was washed and peeled, dried in the oven to a steady weight and then ground into milled powder. The powder was extracted with ethanol at a ratio of 1:10 for 48 h, and then heated in a thermostatic water bath at 60 °C for 6 h [44]. The extract was filtered with a filtering machine to obtain the flavonoids of pomelo peel, and then evaporated by rotary evaporation until no ethanol was precipitated. The extract was freeze-dried in a freeze-dryer to obtain the flavonoids of pomelo peel. A certain mass of deionized water was weighed and added to a certain mass of sodium dodecylbenzene sulfonate to prepare an emulsifier solution. A certain mass of teak peel extract was dissolved in a certain mass of ethanol to obtain a core solution. The core solution was slowly added dropwise to the emulsifier solution. The core solution was gradually introduced dropwise to the emulsifier solution. A magnetic stirrer was placed into the solution and stirred continuously at 600 rpm for 40 min in a constant-temperature water bath at 60 °C. The emulsified core emulsion was obtained.

(3) Microcapsule covering and shaping: The wall prepolymer was gradually dropped into the core emulsion using a dropper with a rubber tip at a certain speed. The pH of the solution was readjusted to about 3 by the addition of citric acid monohydrate. The water temperature was controlled, and the solution was heated and reacted in a constant-

temperature water bath for 3 h. The solution was left to precipitate for 36 h at room temperature, then rinsed through a filtering machine using ethanol and water. The obtained product was put into an oven at 50 °C, dried for 24 h, and then milled, and the resulting powder was melamine resin-covered pomelo peel flavonoid antibacterial microcapsules.

2.3. Paint Film Preparation Method

In this experiment, waterborne topcoats with different contents of microcapsules were coated onto silicone molds and glass panels to test the different properties of the waterborne acrylic paint films and to analyze the influence of different contents of microcapsules on the paint films. According to the manual finishing method, the common content of coating is 60 g/m^2–80 g/m^2 with 4–6 layers. In order to simulate the routine use of the coating on the substrate surface and the loss in actual use, the average amount of paint film applied per piece was set at 400 g/m^2 with a thickness of about 80 μm. The material details of the waterborne paint films are listed in Table 5.

Table 5. List of waterborne paint film materials.

Content of the Microcapsules (%)	Microcapsule Weight (g)	Waterborne Coating Weight (g)
0	0	1.00
3.0	0.03	0.97
6.0	0.06	0.94
9.0	0.09	0.91
12.0	0.12	0.88
15.0	0.15	0.85

The optimal samples of microcapsules prepared in single-factor test were added to waterborne acrylic topcoat with different contents of 3.0%, 6.0%, 9.0%, 12.0%, and 15.0%, respectively, and compared with the blank samples of waterborne paint film without microcapsules. Microcapsules were mixed with the waterborne coating, coated in the silicone mold, and left to level for 1 h at room temperature. The paint film was dried in an oven at 50 °C for 30 min to cure. A complete sample was obtained, and the same paint film was coated on a glass plate for testing differences in properties.

2.4. Testing and Characterization

2.4.1. Microencapsulation Yield and Coverage Rate

The microcapsules were dried until their weight no longer changed; then, their weight was recorded, and the weight of the resulting microcapsules calculated as a percentage of the weight of the raw material was the yield rate of the microcapsules.

A certain mass of microcapsule powder was weighed and recorded as M_1, the microcapsule powder was fully ground until the microcapsule wall material was damaged, the ground powder was fully immersed in anhydrous ethanol for 2 d, and then anhydrous ethanol was added again for 4 h to completely dissolve the core material. After completion of immersion, filtration was carried out, and the filtered core material was rinsed repeatedly with deionized water and ethanol. The product obtained from filtration was allowed to dry in an oven at 50 °C until at a constant weight, and the obtained product was the residual wall material, which was recorded as M_2. The coverage rate (P) of the microcapsules was calculated according to Equation (1).

$$P = (M_1 - M_2)/M_1 \times 100\% \quad (1)$$

2.4.2. Characterization of Morphology and Chemical Composition

The micromorphology of the microcapsules was observed and analyzed using an optical microscope with a 20× lens and a scanning electron microscope. The microscopic morphology of the paint film was characterized by scanning electron microscopy. The

chemical composition of the microcapsules and paint film was tested and characterized using an infrared spectrometer, and the microcapsule powder was made into thin flakes for infrared testing by means of a powder compactor.

2.4.3. Paint Film Antibacterial Experiment

The antibacterial experiment for waterborne paint film was conducted on two strains of *Escherichia coli* and *Staphylococcus aureus* according to GB/T 21866-2008 [46]. Activation of the strains was carried out first. Plane nutrient agar medium was prepared by dissolving nutrient agar medium powder in purified water, and fresh strains were transferred to flat nutrient agar medium and placed at 37 °C and 95% humidity for incubation.

Preparation of bacterial suspension was then carried out. Sodium chloride was taken into water to prepare an eluent with a concentration of 0.85%. The inoculation ring was used to take 1–2 rings of fresh bacteria to add to the broth nutrient solution, and was sequentially diluted in 10-fold increments, according to GB/T 4789.2-2016 [47], to make 1:1000 bacterial suspension. The bacterial suspension was dropped onto the paint film, which was then covered with polythene film. The samples were incubated in a humidity chamber at 95% and 37 °C for 24 h, with three parallel tests required for every sample.

After the sample was removed, the sample and cover film were rinsed repeatedly with 20 mL of elution solution. The eluate was stirred well and then 0.5 mL of the eluate was inoculated into flat nutrient agar medium and incubated at 95% humidity and 37 °C for 48 h in a constant temperature and humidity chamber for viable bacteria counting. The colony counter was used to record the number of colonies in the flat nutrient agar medium. The average of 3 groups of parallel tests is the colony number of the sample, and the result of the colony number multiplied by 1000 is the actual value of viable bacteria recovered from each sample after 48 h of incubation. The antibacterial rate of the paint film was calculated as according to Equation (2). The antibacterial rate (R) was calculated with the average number of recovered colonies (B) after 48 h of the paint film without microcapsules, and the average number of recovered colonies (C) after 48 h of the paint film with microcapsules; the unit is cfu/piece.

$$R = (B - C)/B \times 100\% \quad (2)$$

2.4.4. Paint Film Optical Property Test

According to GB/T 11186.3-1989 [48], a portable color difference meter was utilized to assess the color difference of the paint film. After calibrating the color difference meter, a point on the paint film was selected for testing, and the L, a, and b chromaticity values of the paint film were recorded. Three points were selected for each paint film to be tested, and the average value was calculated as the chromaticity value of the paint film. The value L is the lightness or darkness of the measured paint film; the larger the value L, the brighter the color of the paint film. The value a is the color change in red–green color, where a positive value means that the paint film shows red color and a negative value means that the paint film shows green color. The value b is the color change in yellow–blue color, where a positive value means that the paint film appears yellow and a negative value means that the paint film appears blue. The test values for paint films without microcapsules are denoted as L_1, a_1, and b_1, and those with microcapsules are denoted as L_2, a_2, and b_2. The color difference ΔE of the paint film is determined using Equation (3), where $\Delta L = L_2 - L_1$; $\Delta a = a_2 - a_1$; $\Delta b = b_2 - b_1$.

$$\Delta E = \left[(\Delta L)^2 + (\Delta a)^2 + (\Delta b)^2\right]^{1/2} \quad (3)$$

According to GB/T 4893.4-2013 [49], the glossiness of the paint film was tested by using a touch-screen three-angle glossmeter, and the glossiness of the paint film was determined at 20°, 60°, and 85° incidence angles, respectively. The loss of gloss (G_L) in the paint film at 60° incidence angle was calculated according to Equation (4); G_0 is the gloss

of the paint film without microcapsules added and G_1 is the gloss of the paint film with microcapsules added.

$$G_L = (G_0 - G_1)/G_0 \times 100\% \quad (4)$$

The transmittance of the paint film was tested using a UV spectrophotometer in the visible wavelength range of 380 nm–780 nm. The transmittance is the ratio of the remaining light intensity to the incident light after a beam of light passes through a sample.

2.4.5. Mechanical Properties of Paint Films

Tensile testing of the paint film was carried out using a universal mechanical testing machine, in which the paint film was prepared as a standard sample of a certain thickness, width, and length, and a fixture was attached to carry out the test. The results of the test were used to draw the stress–strain curve, and Equation (5) was used to calculate the elongation at break (e) at the point of fracture. The initial length of the paint film was recorded as L_0. When the paint film broke, the increased length was recorded as L. The ratio of the increased length to the initial length was the elongation at break (e) at the point of fracture.

$$e = L/L_0 \times 100\% \quad (5)$$

The roughness of the paint film was tested using a fine roughness tester by placing the sample on a test bench and adjusting a diamond probe with a needle tip curvature radius of approximately 2 microns to make contact with the sample.

There were four repetitions of all tests, all within 5% error.

3. Results and Discussion

3.1. Analysis of the Yield and Coverage Rate of the Microcapsules

In the preparation of microcapsules, when the yield is too low, it may lead to increased cost, low efficiency, and even affect their application. And when the yield is too high, although it can improve productivity, it may also lead to a decline in microcapsule quality, such as the particle size being too large, the wall too thick, the forming rate low, the adhesion strong, and other problems. Thus, it is necessary to analyze microcapsule preparation results by combining a variety of factors. In microcapsule preparation, the level of yield has a direct effect on the results of microcapsule preparation. The yield rate of the microcapsules from orthogonal tests is listed in Table 6. Through the four-factor, three-level orthogonal test, it was concluded that among the nine microcapsule samples, Sample 8 had the highest yield rate with a result of 66%, followed by Sample 6 with a result of 61%. From analysis of the extreme differences in results, it can be concluded that the effect of the four factors on the yield rate is in the order B > A > D > C, so the biggest influence on yield rate is factor B, that is, the microcapsule preparation reaction temperature, followed by the mass ratio of core to wall materials, followed by the emulsifier concentration, and finally the stirring speed during the microcapsule reaction. The optimal preparation process for microcapsule yield is A3 B2 C3 D3. In the variance result data, the factors influencing microcapsule yield were basically the same as for the range result, and it could be observed through the quadratic sum data that factor B has the greatest influence on yield, and to a much larger extent than the other three factors. Therefore, it can be concluded that factor B has the greatest effect on yield rate, and the optimum process for preparation is a 0.12:1 mass ratio of core to wall material, microcapsule reaction stirring speed of 1000 rpm, and emulsifier concentration of 3%.

Table 6. Analysis of microcapsule yield rate results.

Item	Sample	Factor A $m_{(core\ material)}$: $m_{(wall\ material)}$	Factor B Temperature (°C)	Factor C Stirring Speed (rpm)	Factor D Emulsifier Concentration (%)	Yield Rate (%)
Analysis of range	1	0.08:1	50	600	1	48
	2	0.08:1	60	800	2	58
	3	0.08:1	70	1000	3	55
	4	0.10:1	50	800	3	54
	5	0.10:1	60	1000	1	61
	6	0.10:1	70	600	2	53
	7	0.12:1	50	1000	2	57
	8	0.12:1	60	600	3	66
	9	0.12:1	70	800	1	55
	Mean value 1	53.667	53.333	55.667	54.667	
	Mean value 2	56.000	61.667	55.667	56.000	
	Mean value 3	59.333	54.333	57.667	58.333	
	Range	5.666	8.667	2.000	3.666	
	Primary and secondary order	B > A > D > C				
	Optimal level	A3	B2	C3	D3	
	Optimal scheme	A3 B2 C3 D3				
Analysis of variance	Quadratic sum	48.667	130.667	8	20.667	
	Free degree	2	2	2	2	
	F-ratio	0.936	2.513	0.154	0.397	
	F-critical value	4.640	4.640	4.640	4.640	
	Significance					

The coverage rate is also one of the important indexes for measuring the results of microcapsule preparation, which refers to the mass ratio of the core material covered by the microcapsule to the whole microcapsule. Table 7 shows the analysis of the range and variance results of the coverage rate of the microcapsules prepared in the orthogonal test. The highest coverage rate was found in Sample 9, up to 21%. According to the analysis of the extreme deviation results, it can be concluded that the effect of the four factors on the microcapsule coverage rate is in the order B > C > A > D, so the biggest influencing factor of microcapsule coverage rate is B, that is, the reaction temperature in the preparation of microcapsules, followed by the stirring speed of the microcapsule reaction, followed by mass ratio of core to wall material, and finally the concentration of emulsifiers. The optimal preparation process for microcapsule coverage rate is A3 B3 C2 D2. In the variance result data, the factors influencing microcapsule coverage rate were basically the same as for the range result, and it could be observed through the quadratic sum data that the influence of factor B on the microcapsule coverage rate is much larger than that of the other three factors.

An in-depth study of the key factors in the microcapsule preparation process was carried out by orthogonal tests, and the results indicated that the reaction temperature was the most significant influence on the melamine resin-covered pomelo peel flavonoid microcapsules during microcapsule preparation. Orthogonal testing is an experimental design method that utilizes the nature of orthogonal tables to reduce the number of trials and increase their efficiency by combining multi-factor, multi-level trials into a small number of representative trial combinations. The purpose of the test is to find out what effects the factors have, which are major, and which are minor, so as to determine the most suitable production conditions. In orthogonal experimental design, factors can be quantitative or qualitative. And the distance between levels of quantitative factors can be equal or unequal. In terms of yield rate, the optimal combination of process

parameters was a core-to-wall material mass ratio of 0.12:1, reaction temperature of 60 °C, stirring speed of 1000 rpm, and emulsifier concentration of 3%. For the coverage rate, the optimal combination of process parameters was obtained as a 0.12:1 mass ratio of core to wall material, reaction temperature of 70 °C, stirring speed of 800 rpm, and emulsifier concentration of 2%. The largest influencing factor in both yield rate and coverage rate results was the reaction temperature, so the reaction temperature was used as a variable to further optimize the microcapsule preparation process in the single-factor tests. The morphology of the microcapsules shows that when the rotational speed of the microcapsule reaction is high, it may lead to microcapsule rupture and serious agglomeration and adhesion, and when the rotational speed is low, the microcapsule size is small. Thus, 800 rpm was used as the stirring speed of the microcapsule reaction in the single-factor tests. A high coverage rate represents a higher content of core material in the microcapsules, which helps to improve their antibacterial properties, so the microcapsule core was selected to be emulsified with a 2% concentration of emulsifier from the microcapsule coverage rate result for the single-factor tests. This finding provided an important basis for optimizing the microcapsule preparation process.

Table 7. Analysis of microcapsule coverage rate results.

Item	Sample	Factor A $m_{(core\ material)}$: $m_{(wall\ material)}$	Factor B Temperature (°C)	Factor C Stirring Speed (rpm)	Factor D Emulsifier Concentration (%)	Coverage Rate (%)
Analysis of range	1	0.08:1	50	600	1	10
	2	0.08:1	60	800	2	15
	3	0.08:1	70	1000	3	14
	4	0.10:1	50	800	3	13
	5	0.10:1	60	1000	1	12
	6	0.10:1	70	600	2	20
	7	0. 12:1	50	1000	2	11
	8	0. 12:1	60	600	3	15
	9	0.12:1	70	800	1	21
	Mean value 1	13.000	11.333	15.000	14.333	
	Mean value 2	15.000	14.000	16.333	15.333	
	Mean value 3	15.667	18.333	12.333	14.000	
	Range	2.667	7.000	4.000	1.333	
	Primary and secondary order	B > C > A > D				
	Optimal level	A3	B3	C2	D2	
	Optimal scheme	A3 B3 C2 D2				
Analysis of variance	Quadratic sum	11.556	74.889	24.889	2.889	
	Free degree	2	2	2	2	
	F-ratio	0.405	2.623	0.872	0.104	
	F-critical value	4.460	4.460	4.460	4.460	
	Significance					

The results of yield rate and coverage rate from the orthogonal tests were combined, and the single-factor tests were designed with reaction temperature as the variable, a 0.12:1 mass ratio of core to wall material, stirring speed of 800 rpm, and emulsifier concentration of 2%. The results of the single-factor tests for microencapsulation are listed in Table 8. The microcapsule yield increased gradually with the increase in temperature when the reaction temperature was below 60 °C, and the highest yield rate was 51% when the microcapsule reaction temperature reached 60 °C. When the microcapsule reaction temperature was higher than 60 °C, the yield decreased gradually with the increase in temperature. This could be due to the reaction temperature being too high, preventing the microcapsule walls

from forming fully, resulting in lower yields. The microcapsule coverage rate gradually increased with the increase in temperature, and the highest coverage rate was 22% at 80 °C, but the results at each reaction temperature were relatively similar. Therefore, by combining the yield, reaction temperature, and morphology of the microcapsules in the single-factor tests, the reaction temperature of 60 °C was selected as the optimal preparation process parameter, i.e., Sample 12. The application of the microcapsules was further investigated by adding them to waterborne coatings. Therefore, analyzing the results of orthogonal and single-factor tests for the preparation of microcapsules, the preferred microcapsule preparation process in this experiment was a 0.12:1 mass ratio of core to wall material, reaction temperature of 60 °C, stirring speed of 800 rpm, and emulsifier concentration of 2%.

Table 8. Results of single-factor experiments on microencapsulation.

Sample	Temperature (°C)	Yield Rate (%)	Coverage Rate (%)
10	40	45	16
11	50	47	17
12	60	51	20
13	70	46	20
14	80	42	22

3.2. Morphological Analysis of Microcapsules

The macroscopic morphology of the flavonoids of pomelo peel core material, melamine resin wall material, and microcapsule samples prepared is shown in Figure 2. It can be observed that the core material comprised yellow crystals, the wall material was beige powder, and the obtained microcapsules were in the form of a yellowish powder. This is because in the process of microcapsule preparation, the yellow core material was covered by the beige melamine resin wall material, the core material stained the wall material, and at the same time, the wall material of the microcapsule was also thinner and had very small pores, which released the color of the core material. It can be tentatively demonstrated that the successfully prepared microcapsules contained both pomelo peel flavonoids and melamine resin.

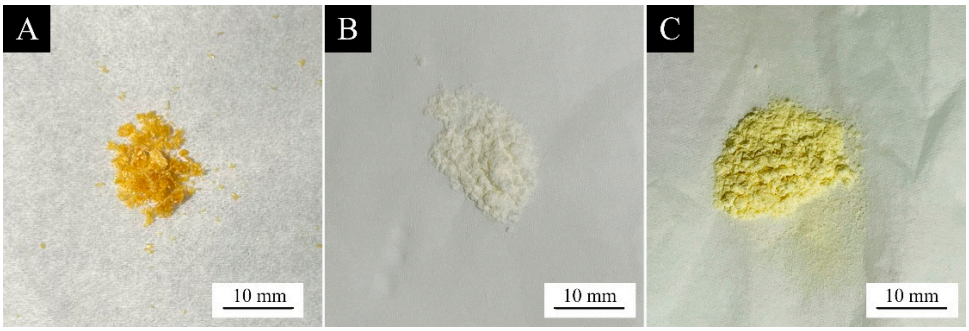

Figure 2. Macromorphology: (**A**) core material (pomelo peel flavonoids), (**B**) wall material (melamine resin), and (**C**) melamine resin-covered pomelo peel flavonoid microcapsules.

Microscopic images of the microcapsules are shown in Figures 3 and 4. It became clear from the microscopic photographs that there were two kinds of different media in the microcapsules, which initially proved that the prepared microcapsules had two different substances, namely, a wall material and core material, where the internal bright spot represents the core material, pomelo peel flavonoids. According to the observation, it can be found that the microcapsules prepared for Sample 2 at 800 rpm in the orthogonal test had the best dispersion, the least agglomeration, and more uniform dispersion. The microcapsules prepared for Sample 3, Sample 5, and Sample 7 at 1000 rpm had more serious agglomeration and adhesion. Sample 1, Sample 6, and Sample 8 were prepared at

600 rpm with relatively fewer microcapsules. Therefore, the preparation parameters using a stirring speed of 800 rpm during the reaction were selected to optimize the microcapsule preparation process in the single-factor tests.

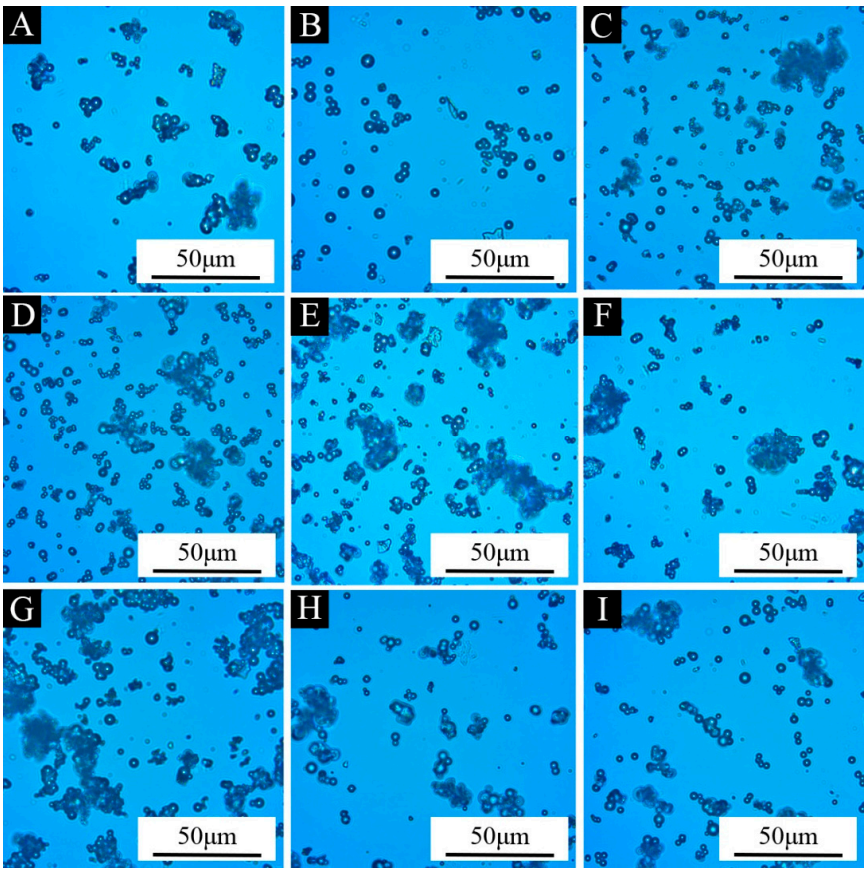

Figure 3. OM images of microcapsules in the orthogonal test: (**A**) Sample 1, (**B**) Sample 2, (**C**) Sample 3, (**D**) Sample 4, (**E**) Sample 5, (**F**) Sample 6, (**G**) Sample 7, (**H**) Sample 8, (**I**) Sample 9.

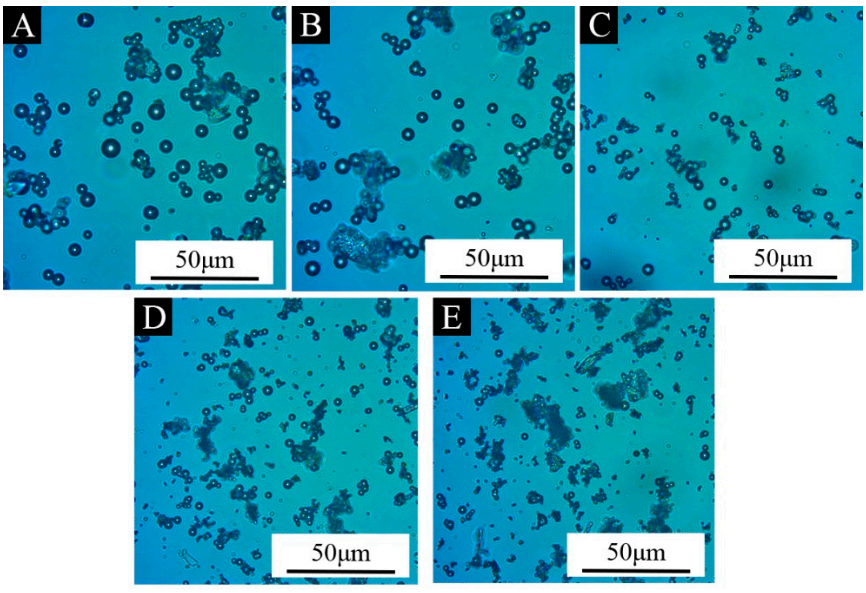

Figure 4. OM images of microcapsules in the single-factor tests: (**A**) Sample 10, (**B**) Sample 11, (**C**) Sample 12, (**D**) Sample 13, and (**E**) Sample 14.

According to the microcapsule microscopy of the single-factor samples, the microcapsule samples gradually became smaller in particle size with increasing temperature, and the agglomeration and adhesion phenomenon was gradually aggravated, and the microcapsule samples prepared at the reaction temperature of 80 °C of Sample 14 had the most serious agglomeration phenomenon, and the fewest microcapsules were formed. This may be due to the increase in temperature, resulting in an acceleration in reaction rate, so that the excess wall material deposition results in the formation of amorphous agglomerations. The microcapsule samples with a reaction temperature below 80 °C were well formed with a bright and clean surface, as shown in Figure 5.

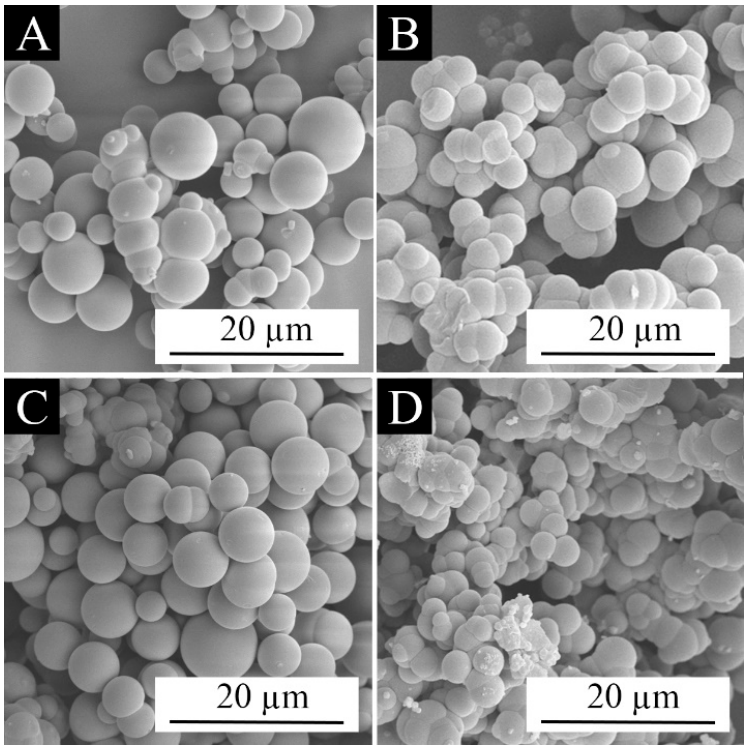

Figure 5. SEM images of microcapsules in the single-factor tests: (**A**) Sample 10, (**B**) Sample 11, (**C**) Sample 12, and (**D**) Sample 13.

Figure 6 shows the particle size distribution of microcapsules in single-factor tests. As can be seen from Figure 6A,B, when the microcapsule reaction temperature is relatively low, the microcapsule particle size is larger, mainly distributed between 3 and 8 μm, and the microcapsule with the largest particle size distribution is mainly concentrated at around 5–7 μm. From Figure 6C, it can be seen that the particle size distribution of the microcapsules of Sample 12 is smaller and more homogeneous, mostly distributed between 1 and 6 μm, and the microcapsules with the largest particle size distribution are mainly concentrated at about 2–3 μm. From Figure 6D, it can be seen that the microcapsule particle size is mainly distributed between 2 and 7 μm, more dispersed, which indicates the different sizes and uneven distribution. It can be seen that Sample 12 microcapsules have the most uniform particle size distribution.

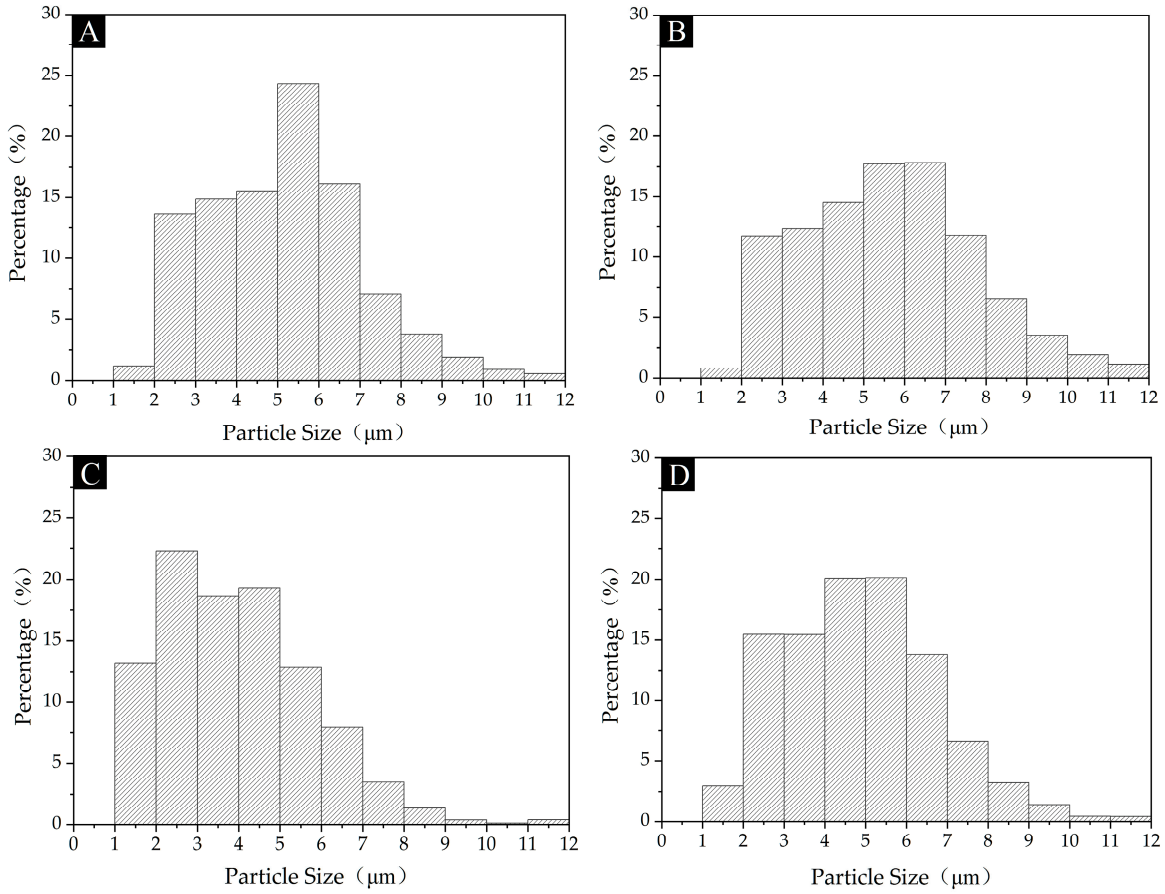

Figure 6. Particle size distribution of microcapsules in the single-factor experiment: (**A**) Sample 10, (**B**) Sample 11, (**C**) Sample 12, and (**D**) Sample 13.

3.3. Analysis of the Morphology of the Paint Films

The macroscopic morphology pictures of paint films with different contents of microcapsules are shown in Figure 7. The paint film without melamine resin-covered pomelo peel flavonoid microcapsules is colorless and clear, and the paint film with added microcapsules is beige in color. The transparency of the paint film gradually decreases with the increase in microcapsule content, which is because the dense amine resin is white and the of pomelo peel flavonoids are yellow. Thus, the microcapsule powder that is successfully covered is beige, and it is added to the transparent and colorless waterborne paint, which results in the transparency of the paint film as the content changes. From Figure 7B,C, it can be found that when the content of microcapsules added is less than 9.0%, the paint film is still transparent. From Figure 7D–F, it can be observed that when the content of microcapsules added is 9.0% and above, the transparency of the paint film is obviously reduced, the particles on the surface of the paint film are increased, and a cracking phenomenon occurs. Figure 7E shows that when the microcapsule content reaches 12.0%, large cracks begin to appear at edge of the paint film. This is because the microcapsule content is too high, resulting in a reduction in the content of waterborne coating and leveling deterioration, which indicates that when the microcapsule content is more than 9.0%, it is not suitable for application in practice.

Figure 8 shows the microscopic morphology of the paint film with 0%, 3.0%, 6.0%, and 9.0% of melamine resin-covered pomelo peel flavonoid microcapsules. The surface of the paint film without the addition of microcapsules is flat and smooth, and when the number of microcapsules added is 3.0% and 6.0%, the surface of the paint film appears to have a slight granularity. When the addition of microcapsules reaches 9.0%, as shown in Figure 8D, in addition to the feeling of particles, there are more clearly visible wrinkles

on the surface of the film, due to there being too many microcapsules, and they cannot be dispersed uniformly in the paint film, resulting in microcapsule agglomeration in the paint film and the formation of large particles on the surface of the paint film. It can be observed that the number of microcapsules above 9.0% has a large adverse influence on the transparency and smoothness of the paint film.

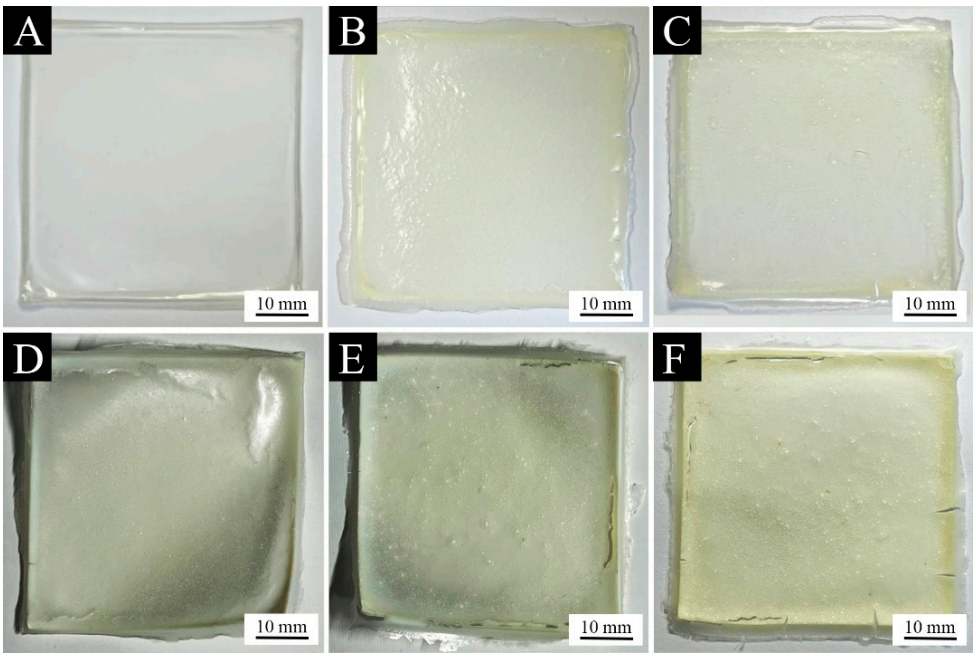

Figure 7. Macromorphology of the paint films: (**A**) paint film with 0% microcapsules, (**B**) paint film with 3% microcapsules, (**C**) paint film with 6% microcapsules, (**D**) paint film with 9% microcapsules, (**E**) paint film with 12% microcapsules, and (**F**) paint film with 15% microcapsules.

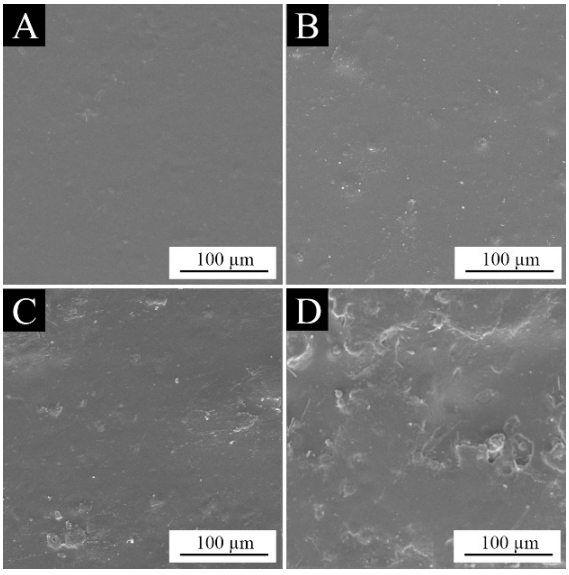

Figure 8. SEM images of the paint films: (**A**) paint film with 0% microcapsules, (**B**) paint film with 3% microcapsules, (**C**) paint film with 6% microcapsules, and (**D**) paint film with 9% microcapsules.

3.4. Chemical Composition Analysis of Paint Films

Figure 9 shows the infrared spectrum of melamine resin wall material, microcapsule, pomelo peel flavonoid, paint film without microcapsules, and paint film with microcapsules. The absorption peak of the bending vibration of the triazine ring in the melamine resin is at

813 cm^{-1} [50,51]. The absorption peak of C-O is around 1000 cm^{-1}. The absorption peak caused by the stretching vibration of N-H is at 1558 cm^{-1}. These characteristic peaks are present in both the melamine resin wall material and microcapsules, indicating the presence of melamine resin in the microcapsules. The infrared spectrum of pomelo peel extract in the figure has broad and strong absorption peaks formed by mesohydroxyl group conjugation near 3390 cm^{-1}, which indicates the presence of a large number of phenolic hydroxyl groups or hydroxyl groups. Stretching vibrational peaks due to C-O in the pomelo peel extract are near 1646 cm^{-1} and 1058 cm^{-1}. Near 1144 cm^{-1} is the vibrational peak of C-O in the waterborne coating. Near 1726 cm^{-1} is the characteristic peak of C=O [52]. Since the characteristic peaks of C-O and C=O are present in the microcapsules, pomelo peel extract, and waterborne coating, the characteristic peaks in the paint film with added microcapsules are more intense. Thus, it is proven that the chemical composition of melamine resin and pomelo peel extract existed in the microcapsules, and that the chemical components of the microcapsules applied to waterborne coatings were not destroyed.

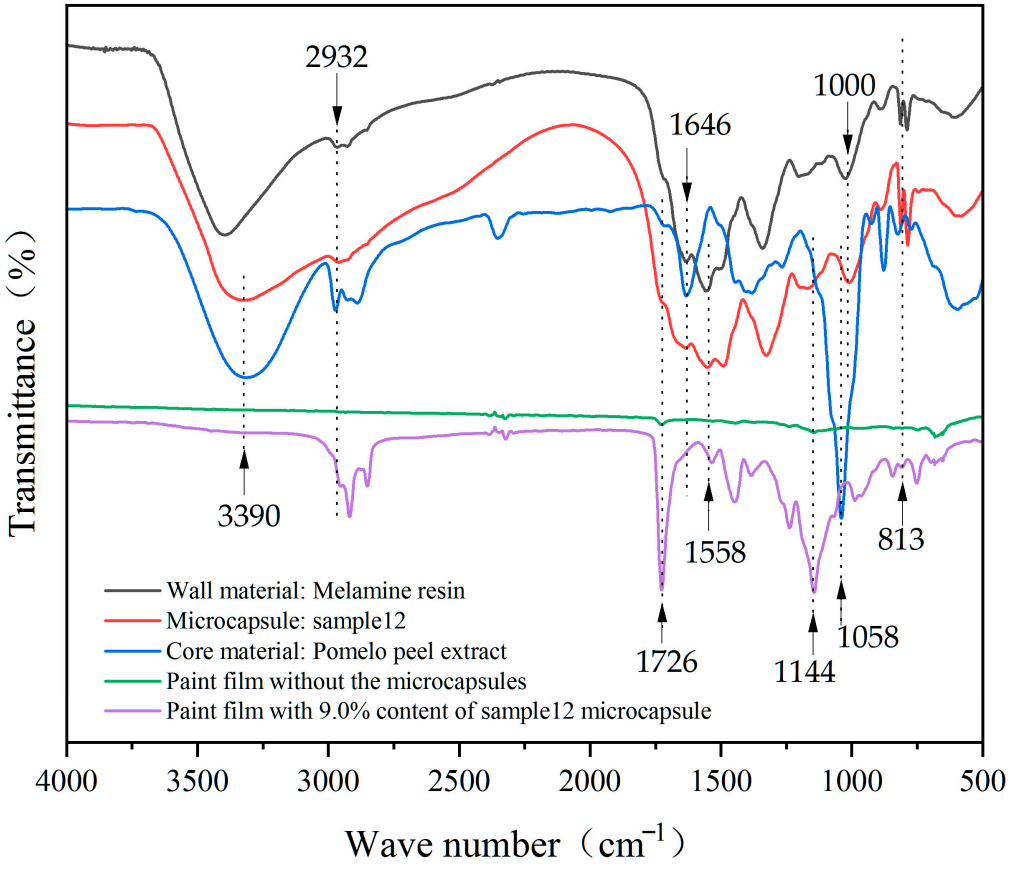

Figure 9. FTIR image of the paint films.

3.5. Analysis of the Effect of Microcapsules with Different Content Levels on the Antibacterial Properties of Paint Films

Table 9 shows the results after antibacterial testing of paint films mixed with different levels of melamine resin-covered pomelo peel flavonoid microcapsules against *Escherichia coli* and *Staphylococcus aureus*, respectively. It can be found that relative to the paint film without microcapsules, the paint film with microcapsules added gradually increased the antibacterial rate against both bacteria with an increase in the added amount, and the antibacterial effect was gradually enhanced, which indicates that the waterborne coatings themselves have a low inhibitory effect on the growth of bacteria. The addition of microcapsules increased the inhibitory effect of the paint film on bacteria, and the antibacterial rate can reach a maximum of 72.1% and 85.0%, respectively. It can be seen that the melamine resin-covered pomelo peel flavonoid microcapsules in the paint film have

antibacterial properties. As shown in Figure 10, the antibacterial properties of the microcapsules against *Staphylococcus aureus* were slightly higher than those against *Escherichia coli*, and the incorporation of the microcapsules acted as an antibacterial agent for the paint film.

Table 9. Antibacterial rate of the paint films with different microcapsule loadings.

Microcapsule Content (%)	Average Number of Recovered *Escherichia coli* (CFU·Piece^{-1})	Antibacterial Rate against *Escherichia coli* (%)	Average Number of Recovered *Staphylococcus aureus* (CFU·Piece^{-1})	Antibacterial Rate against *Staphylococcus aureus* (%)
0	190	-	432	-
3.0	143	24.7	316	26.9
6.0	113	40.5	214	50.5
9.0	87	54.2	138	68.1
12.0	68	64.2	97	77.6
15.0	53	72.1	65	85.0

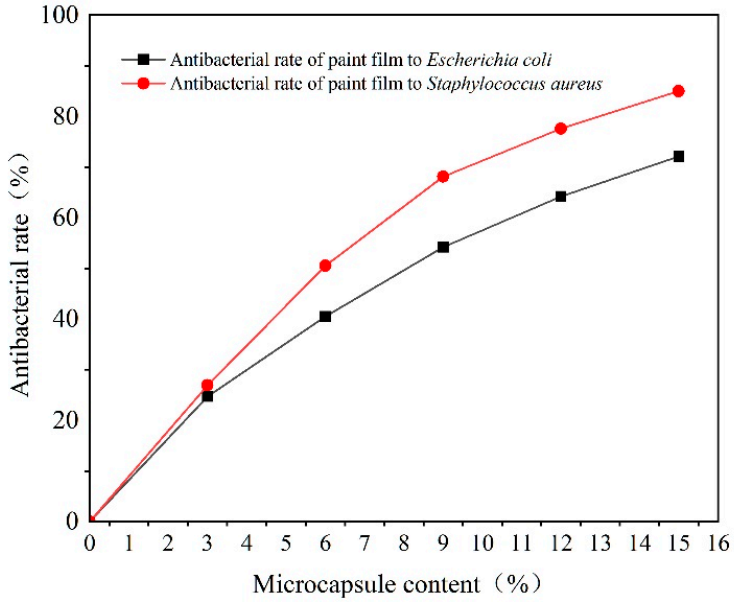

Figure 10. Antimicrobial rate of paint films with different contents of microcapsules against *Escherichia coli* and *Staphylococcus aureus*.

This proves that the encapsulation of microcapsules can effectively avoid that the core material too easily dissolves in the waterborne coating, improve the stability, and successfully retain the original antibacterial properties. After the microcapsules were filtered and dried, the water, ethanol, and other solvents evaporated; the microcapsules were covered and shaped; and the walls formed microvoids, through which the core material, pomelo peel flavonoids, had an inhibitory effect on the growth of *Escherichia coli* and *Staphylococcus aureus* in the waterborne paint film.

3.6. Analysis of the Effect of Microcapsules with Different Content Levels on the Optical Properties of Paint Films

The chromaticity values of and color differences in the paint films are listed in Table 10. The color difference value of the paint film becomes higher gradually with the addition of microcapsules. The *L* value, which represents the lightness or darkness of the paint film, is opposite to the color difference and decreases gradually with the increase in microcapsule content, which is due to the fact that the beige, granular powder of the melamine resin microcapsules does not react with the transparent waterborne coating. It maintains the particle state and deepens the color of the paint film. Thus, the color and flatness of the

paint film itself are affected by the added content of the microcapsules. The *b* value of the paint film, which represents the greenish yellow value, is negative when the content of microcapsules is 6.0% or less, indicating that the color of the paint film is bluish, which is due to the transparent color of the paint film itself, and when the content of microcapsules is less, it has less influence on the greenish yellow value of the paint film. When the *b* value of the paint film is positive, it means that the color of the paint film is yellowish, when the content of microcapsules in the paint film is more than 6.0%, with the increase in the content of microcapsules, the yellow degree of the paint film gradually deepens; this is because the microcapsules are beige in color, which has an effect on the color of the paint film.

Table 10. Chromaticity and color difference values of paint films at different microcapsule addition contents.

Microcapsule Content (%)	*L*	*a*	*b*	Δ*E*
0	81.91	1.73	−2.27	-
3.0	79.47	1.10	−1.43	2.66
6.0	78.94	1.10	−1.03	3.28
9.0	78.43	0.93	0.67	4.63
12.0	76.10	0.63	0.97	6.74
15.0	73.23	0.54	1.36	9.48

The paint film gloss and gloss loss data are listed in Table 11. As the contents of the microcapsules increased, the paint film gloss at 20°, 60°, and 85° angle of incidence was gradually reduced. The gloss loss rate of the paint film at 60° incidence angle gradually increased with the increase in microcapsule content; when the microcapsule content was 15.0%, the gloss loss rate of the paint film was as high as 71.3%. This is because the granular melamine resin microcapsules affect the smoothness of the paint film after drying, and when the content of the microcapsules increases, the surface of the paint film gradually becomes rougher, which produces a diffuse reflection of the light, resulting in a reduction in gloss and an increase in gloss loss rate.

Table 11. Gloss and gloss loss rate of paint films at different microcapsule addition content levels.

Microcapsule Content (%)	20° (%)	60° (%)	85° (%)	Gloss Loss Rate (%)
0	6.10	17.45	31.17	-
3.0	2.80	9.13	3.77	47.7
6.0	2.57	8.67	2.63	50.3
9.0	2.17	7.07	1.43	59.5
12.0	1.67	5.43	0.83	68.9
15.0	1.53	5.00	0.77	71.3

Figure 11 displays the transmittance of paint film with varying microcapsule contents, and the transmittance of the paint film decreases gradually with the increase in microcapsule content. This is because the beige microcapsules, when added to colorless and transparent waterborne coating, reduces the transparency of the paint film and has an effect on the light transmission. The visible wavelength range of the paint film tested is 380 nm–780 nm. From Figure 11, it can be clearly seen that although the transmittance of the paint film with microcapsules is lower than that of the paint film without microcapsules, the transmittance of the paint film with different microcapsule contents tends to be relatively transmissive, showing a smooth width of the visible wavelength band. This is due to the lighter color of the melamine resin-covered pomelo peel flavonoid microcapsules, which has less effect on the visible light transmittance of the paint film when added, making it suitable for practical application.

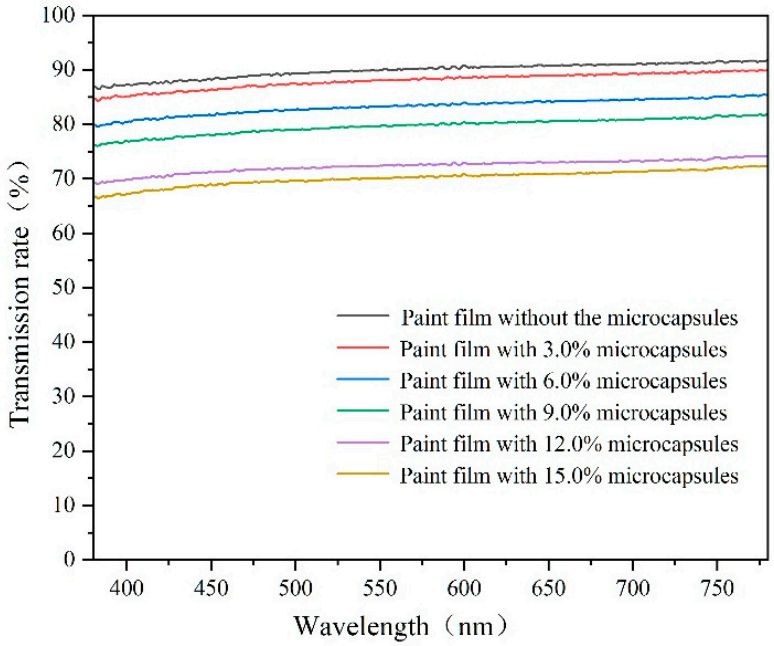

Figure 11. Light transmittance trend of paint films with different microcapsule addition content levels.

3.7. Effect of Microcapsules with Different Content Levels on the Mechanical Properties of Paint Films

The impact of various microcapsule content levels on the tensile properties of paint films are shown in Figure 12. The elastic region of the paint film was greatest when there were no microcapsules in the paint film, indicating that the waterborne paint film itself had great ductility. When the microcapsule content is between 3.0% and 9.0%, the paint film also has some stretching areas that decrease with increasing content. This is due to the fact that the melamine resin-covered pomelo peel flavonoid microcapsules were distributed in the coatings, increasing the density of the coatings and thus reducing the ductility of the waterborne paint film itself. When the microcapsule content is higher than 12.0%, the stretching area of the paint film decreases sharply. When the paint film contains 15.0% microcapsules, the tensile area of the paint film becomes very small, and then the strain of the paint film under high stress is very small, which indicates that the paint film is very hard and has low ductility. This is because the high content of microcapsules enhanced the hardness of the paint film, which makes the paint film brittle and reduces its ductility.

Table 12 shows the elongation at break of paint films with different microcapsule addition contents. The elongation at break of the paint film decreases with the increase in microcapsules. The elongation at break of the paint film without microcapsules was 18.9%, and the change in elongation at break of the paint film was lower when the number of microcapsules added was lower than 9.0%. When the number of microcapsules added was as high as 15.0%, the elongation at break of the paint film decreased to 3.8%. This is due to the fact that the larger number of microcapsules resulted in a much less elastic paint film.

Table 12. Paint film elongation at break with different microcapsule content levels.

Microcapsule Content (%)	Elongation at Break (%)
0	18.9
3.0	12.7
6.0	10.8
9.0	10.2
12.0	7.9
15.0	3.8

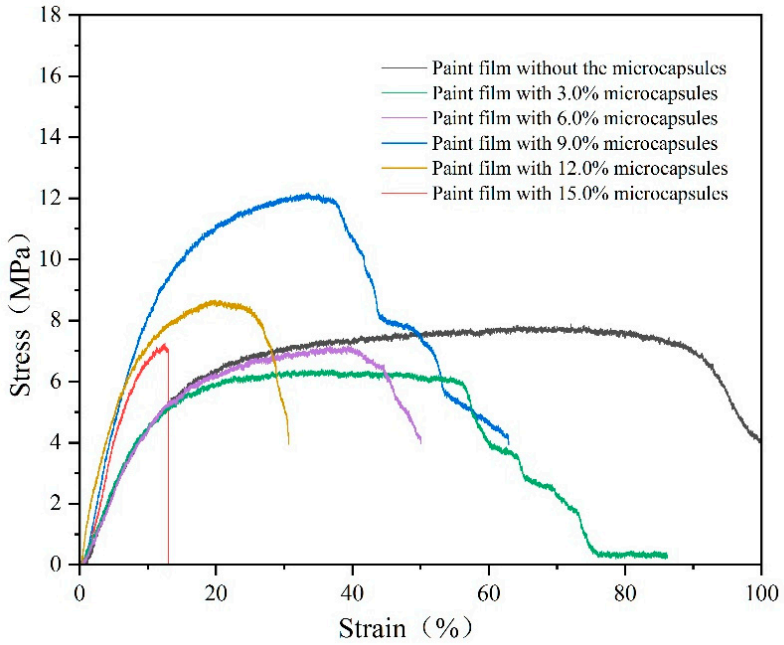

Figure 12. Stress–strain curves of paint films with different microcapsule content levels.

The surface roughness of the paint films at different microcapsule additions is shown in Table 13. The roughness of the paint film increases with the addition of microcapsule content. This is due to the fact that the prepared microcapsules are in the form of tiny spherical particles, which are added to waterborne coatings and prepared into paint films after drying. The incorporation of microcapsules results in the presence of granularity on the surface of the paint film, and as the microcapsule content increases, the paint film's surface roughness also increases.

Table 13. Paint film roughness with different microcapsule content levels.

Microcapsule Content (%)	Roughness (μm)
0	0.27
3.0	0.84
6.0	1.75
9.0	2.97
12.0	3.90
15.0	3.97

4. Conclusions

The best preparation method for melamine resin-covered pomelo peel flavonoid microcapsules was explored by orthogonal test and single-factor tests. The optimum microcapsule was found to be Sample 12. The mass ratio of core to wall material was 0.12:1. The reaction temperature was 60 °C. The stirring speed during the reaction was 800 rpm. The emulsifier concentration was 2%. The antibacterial rate of the paint film against *Escherichia coli* and *Staphylococcus aureus* gradually increased with the increase in microcapsule content, and the maximum reached was 72.1% and 85.0%, respectively. As the content of microcapsules in the paint film increased, the color difference in the paint film gradually became larger, with a maximum of 9.48. The gloss of the paint film then decreased gradually with the increase in microcapsule content, while the light loss rate became larger and the light transmission rate decreased gradually. The tensile properties and elongation at break of the paint film decreased gradually with the increase in microcapsule content, and the lowest elongation at break of the paint film was 3.8% at the highest microcapsule content. The roughness of the paint film gradually became larger with the increase in

microcapsule content. Comprehensive analysis of the test results showed that when the content of microcapsules in the paint film exceeded 9.0%, the film was no longer suitable for application in practice. When the microcapsule content was 6.0%, the paint film had better comprehensive performance. At that time, the antibacterial rate of the paint film against *Escherichia coli* and *Staphylococcus aureus* was 40.5% and 50.5%, respectively; the color difference was 3.28, and it had certain elasticity area; the elongation at break was 10.8%; and the roughness was 1.75 μm. The results expand the application field of waterborne coatings and provide reference values for the antibacterial research of waterborne coatings.

Author Contributions: Conceptualization, methodology, validation, resources, data management, supervision, T.D.; writing—review and editing, formal analysis, investigation X.Y. All authors have read and agreed to the published version of the manuscript.

Funding: This project was partly supported by the Natural Science Foundation of Jiangsu Province (BK20201386).

Institutional Review Board Statement: Not applicable.

Informed Consent Statement: Not applicable.

Data Availability Statement: Data are contained within the article.

Conflicts of Interest: The authors declare that there are no conflicts of interest.

References

1. Zhou, Y.J.; Xie, C.Y. City garden environment research: Optimal design can improve the therapeutic benefit of therapy garden. *Fresen. Environ. Bull.* **2020**, *29*, 11615–11623.
2. Han, M.J.N.; Kim, M.J. Green environments and happiness level in housing areas toward a sustainable life. *Sustainability* **2019**, *11*, 4768. [CrossRef]
3. Tellnes, L.G.F.; Alfredsen, G.; Flaete, P.O.; Gobakken, L.R. Effect of service life aspects on carbon footprint: A comparison of wood decking products. *Holzforschung* **2020**, *74*, 426–433. [CrossRef]
4. Liu, Y.; Hu, W.; Kasal, A.; Erdil, Y.Z. The State of the Art of Biomechanics Applied in Ergonomic Furniture Design. *Appl. Sci.* **2023**, *13*, 12120. [CrossRef]
5. Hu, W.G.; Liu, Y.; Konukcu, A.C. Study on withdrawal load resistance of screw in wood-based materials: Experimental and numerical. *Wood Mater. Sci. Eng.* **2023**, *18*, 334–343. [CrossRef]
6. Hu, W.; Fu, W.; Zhao, Y. Optimal design of the traditional Chinese wood furniture joint based on experimental and numerical method. *Wood. Res.* **2024**, *69*, 50–59. [CrossRef]
7. Jiao, C.Y.; Shao, Q.; Wu, M.Y.; Zheng, B.; Guo, Z.; Yi, J.M.; Zhang, J.X.; Lin, J.; Wu, S.D.; Dong, M.Y.; et al. 2-(3,4-Epoxy) ethyltriethoxysilane-modified waterborne acrylic resin: Preparation and property analysis. *Polymer* **2020**, *190*, 122196. [CrossRef]
8. Ge, H.W.; Zhang, J.F.; Yuan, Y.; Liu, J.C.; Liu, R.; Liu, X.Y. Preparation of organicinorganic hybrid silica nanoparticles with contact antibacterial properties and their application in UV-curable coatings. *Prog. Org. Coat.* **2017**, *106*, 20–26. [CrossRef]
9. Hu, W.; Zhang, J. Effect of growth rings on acoustic emission characteristic signals of southern yellow pine wood cracked in mode I. *Constr. Build. Mater.* **2022**, *329*, 127092. [CrossRef]
10. Chen, B.; Yu, X.; Hu, W. Experimental and numerical studies on the cantilevered leg joint and its reinforced version commonly used in modern wood furniture. *Bioresources* **2022**, *17*, 3952–3964. [CrossRef]
11. Revuelta, M.V.; Bogdan, S.; Gamez-Espinosa, E.; Deya, M.C.; Romagnoli, R. Green antifungal waterborne coating based on essential oil microcapsules. *Prog. Org. Coat.* **2020**, *151*, 106101. [CrossRef]
12. Liu, Y.; Hu, J.; Wu, Z. Fabrication of coatings with structural color on a wood surface. *Coatings* **2020**, *10*, 32. [CrossRef]
13. Chen, B.; Xia, H.; Hu, W. The design and evaluation of the three-dimensional corner joints used in wooden furniture frames: Experimental and numerical. *Bioresources* **2022**, *17*, 2143–2156. [CrossRef]
14. Chen, C.J.; Kuang, Y.D.; Zhu, S.Z.; Burgert, I.; Keplinger, T.; Gong, A.; Li, T.; Berglund, L.; Eichhorn, S.J.; Hu, L.B. Structureproperty-function relationships of natural and engineered wood. *Nat. Rev. Mater.* **2020**, *5*, 642–666. [CrossRef]
15. Yan, X.X.; Han, Y.; Yin, T.Y. Synthesis of urea-formaldehyde microcapsule containing fluororesin and its effect on performances of waterborne coatings on wood surface. *Polymers* **2021**, *13*, 1674. [CrossRef]
16. Julaeha, E.; Eddy, D.R.; Wahyudi, T.; Ningsih, B.A.; Nurzaman, M.; Permadi, N.; Herlina, T.; Al Anshori, J. Coacervate Microcapsules of Citrus aurantifolia Essential Oil (LOs): Optimization and Their Antibacterial Activity Study. *ChemistrySelect* **2022**, *7*, e202200187. [CrossRef]
17. Hu, W.; Wan, H. Comparative study on weathering durability properties of phenol formaldehyde resin modified sweetgum and southern pine specimens. *Maderas-Cienc. Tecnol.* **2022**, *24*, 17. [CrossRef]
18. Hu, W.; Liu, Y.; Li, S. Characterizing mode I fracture behaviors of wood using compact tension in selected system crack propagation. *Forests* **2021**, *12*, 1369. [CrossRef]

19. Yan, X.X.; Wang, L. Preparation of shellac resin microcapsules coated with urea formaldehyde resin and properties of waterborne paint films for Tilia amurensis Rupr. *Membranes* **2020**, *10*, 278. [CrossRef]
20. Hu, W.; Li, S.; Liu, Y. Vibrational characteristics of four wood species commonly used in wood products. *Bioresources* **2021**, *16*, 7101–7111. [CrossRef]
21. Hu, W.; Chen, B. A methodology for optimizing tenon geometry dimensions of mortise-and-tenon joint wood products. *Forests* **2021**, *12*, 478. [CrossRef]
22. Zhi, L.; Zhang, C.Q.; Liu, Z.Z.; Liu, T.; Dou, X.Y.; Chen, Y.Q.; Ou, R.X.; Wang, Q.W. Flexible decorative wood veneer with high strength, wearability and moisture penetrability enabled by infiltrating castor oil-based waterborne polyurethanes. *Compos. Part B-Eng.* **2022**, *230*, 109502. [CrossRef]
23. Yan, X.X.; Han, Y.; Yin, T.Y. Coating process optimization and self-healing performance evaluation of shellac microcapsules coated with melamine/rice husk powder. *Appl. Sci.* **2021**, *11*, 8373. [CrossRef]
24. Wang, J.J.; Lu, Y.Z.; Chu, Q.D.; Ma, C.L.; Cai, L.R.; Shen, Z.H.; Chen, H. Facile construction of superhydrophobic surfaces by coating fluoroalkylsilane/silica composite on a modified hierarchical structure of wood. *Polymers* **2022**, *12*, 813. [CrossRef] [PubMed]
25. Rosu, L.; Varganici, C.D.; Mustata, F.; Rosu, D.; Rosca, I.; Rusu, T. Epoxy coatings based on modified vegetable oils for wood surface protection against fungal degradation. *ACS Appl. Mater. Inter.* **2020**, *12*, 14443–14458. [CrossRef] [PubMed]
26. Han, S.J.; Chen, Y.P.; Lyu, S.Y.; Chen, Z.L.; Wang, S.Q.; Fu, F. Effects of processing conditions on the properties of paraffin/melamine-urea-formaldehyde microcapsules prepared by in situ polymerization. *Colloids Surf. B* **2019**, *585*, 124046. [CrossRef]
27. Huang, N.; Yan, X.X. Preparation of Aloe-Emodin Microcapsules and Its Effect on Antibacterial and Optical Properties of Water-Based Coating. *Polymers* **2023**, *15*, 1728. [CrossRef] [PubMed]
28. Zheng, S.; Bawazir, M.; Dhall, A.; Kim, H.E.; He, L.; Heo, J.; Hwang, G. Implication of Surface Properties, Bacterial Motility, and Hydrodynamic Conditions on Bacterial Surface Sensing and Their Initial Adhesion. *Front. Bioeng. Biotechnol.* **2021**, *9*, 643722. [CrossRef]
29. Weng, M.; Zhu, Y.; Mao, W.; Zhou, J.; Xu, W. Nano-Silica/Urea-Formaldehyde Resin-Modified Fast-Growing Lumber Performance Study. *Forests* **2023**, *14*, 1440. [CrossRef]
30. Hu, W.; Zhang, J. Bolt-Bearing Yield Strength of Three-Layered Cross-Laminated Timber Treated with Phenol Formaldehyde Resin. *Forests* **2020**, *11*, 551. [CrossRef]
31. Barbaz-Isfahani, R.; Saber-Samandari, S.; Salehi, M. Novel electrosprayed enhanced microcapsules with different nanoparticles containing healing agents in a single multicore microcapsule. *Int. J. Biol. Macromol.* **2022**, *200*, 532–542. [CrossRef]
32. Hu, W.; Liu, N. Comparisons of finite element models used to predict bending strength of mortise-and-tenon joints. *Bioresources* **2020**, *15*, 5801–5811. [CrossRef]
33. Yuan, H.Z.; Li, G.X.; Yang, L.J.; Yan, X.J.; Yang, D.B. Development of melamine-formaldehyde resin microcapsules with low formaldehyde emission suited for seed treatment. *Colloids. Surf. B.* **2015**, *128*, 149–154. [CrossRef] [PubMed]
34. Wang, C.; Yu, J.; Jiang, M.; Li, J. Effect of selective enhancement on the bending performance of fused deposition methods 3D-printed PLA models. *Bioresources* **2024**, *19*, 2660–2669. [CrossRef]
35. Tao, Y.; Yan, X.X. Influence of HLB Value of Emulsifier on the Properties of Microcapsules and Self-Healing Properties of Waterborne Coatings. *Polymers* **2022**, *14*, 1304. [CrossRef]
36. Wang, C.; Zhou, Z. Optical properties and lampshade design applications of PLA 3D printing materials. *Bioresources* **2023**, *18*, 1545–1553. [CrossRef]
37. Das, S.; Das, A.; Bhavya, T.; Nivashini, S.R. Molecular characterisation and antibacterial activity of *Aloe barbadensis miller* on textiles. *J. Text. Inst.* **2020**, *111*, 1116–1122. [CrossRef]
38. Xiong, X.Y.; Li, X.B.; Zhu, Z.F.; Zhang, E.D.; Shi, J.; Lu, M.G. Antibacterial and alkali-responsive cationic waterborne polyurethane based on modification of aloe emodin. *Chem. Res. Chin. Univ.* **2023**, *39*, 266–275. [CrossRef] [PubMed]
39. Ding, L.J.; Wang, H.; Liu, D.; Zheng, Z.N. Surface attachment of natural antimicrobial coatings onto conventional polypropylene nonwoven fabric and its antimicrobial performance assessment. *J. Food. Protect.* **2018**, *81*, 172–177. [CrossRef]
40. Wang, C.; Zhang, C.; Ding, K.; Jiang, M. Immersion polishing post-treatment of PLA 3D printed formed parts on its surface and mechanical performance. *Bioresources* **2023**, *18*, 7995–8006. [CrossRef]
41. Luo, Z.; Xu, W.; Wu, S. Performances of Green Velvet Material (PLON) Used in Upholstered Furniture. *Bioresources* **2023**, *18*, 5108–5119. [CrossRef]
42. Luo, Y.; Xu, W. Optimization of Panel Furniture Plates Rework Based on Intelligent Manufacturing. *Bioresources* **2023**, *18*, 5198–5208. [CrossRef]
43. Wang, C.; Yu, J.; Jiang, M.H.; Li, J.Y. Effect of slicing parameters on the light transmittance of 3D-printed polyethylene terephthalate glycol products. *Bioresources* **2024**, *19*, 500–509. [CrossRef]
44. Aichayawanich, S.; Ngaouwthong, C. Antimicrobial Activity of Crude Extract from Pomelo Peel against Staphylococcus aureus. *Adv. Mat. Res.* **2012**, *550–553*, 1871–1874. [CrossRef]
45. Thavanapong, N.; Wetwitayaklung, P. Comparison of Essential Oils Compositions of Citrus maxima Merr. Peel Obtained by Cold Press and Vacuum Stream Distillation Methods and of Its Peel and Flower Extract Obtained by Supercritical Carbon Dioxide Extraction Method and Their Antimicrobial Activity. *J. Essent. Oil Res.* **2020**, *22*, 71–77.

46. *GB/T 21866-2008*; Test Method and Effect for Antibacterial Capability of Paints Film. Standardization Administration of the People's Republic of China: Beijing, China, 2008.
47. *GB/T 4789.2-2016*; National Food Safety Standard Food Microbiological Examination: Aerobic Plate Count. Standardization Administration of the People's Republic of China: Beijing, China, 2016.
48. *GB/T 11186.3-1989*; Methods for Measuring the Colour of Paint Films. Part III: Calculation of Colour Differences. Standardization Administration of the People's Republic of China: Beijing, China, 1990.
49. *GB/T 4893.4-2013*; Test of Surface Coatings of Furniture. Standardization Administration of the People's Republic of China: Beijing, China, 2013.
50. Zotiadis, C.; Patrikalos, I.; Loukaidou, V.; Korres, D.M.; Karantonis, A.; Vouyiouka, S. Self-healing coatings based on poly(urea-formaldehyde) microcapsules: In situ polymerization, capsule properties and application. *Prog. Org. Coat.* **2021**, *161*, 106475. [CrossRef]
51. An, S.; Lee, M.W.; Yarin, A.L.; Yoon, S.S. A review on corrosion-protective extrinsic self-healing: Comparison of microcapsulebased systems and those based on core-shell vascular networks. *Chem. Eng. J.* **2018**, *344*, 206–220. [CrossRef]
52. Scheiner, M.; Dickens, T.J.; Okoli, O. Progress towards self-healing polymers for composite structural applications. *Polymer* **2016**, *83*, 260–282. [CrossRef]